

**ROTATING WAVES FOR SEMICONDUCTOR
INVERTER RINGS**

By

C.C. Lim

J.M. Pimbley

C. Schmeiser

and

D.W. Schwendeman

IMA Preprint Series # 716

November 1990

Rotating Waves for Semiconductor Inverter Rings

by

C.C. Lim¹, J.M. Pimbley², C. Schmeiser³ and D.W. Schwendeman²

A simple model for the time-dependent behavior of semiconductor inverter circuits is used for an analysis of the dynamics of inverter rings. VLSI applications of inverter rings include flip-flops and ring oscillators. The analysis concentrates on the construction of periodic solutions in the form of rotating waves. Three different approaches are used. First, rotating waves are computed explicitly for a model problem. Second, a Hopf bifurcation theorem for problems with symmetries is employed which guarantees the local existence of branches of rotating wave solutions. Third, software for numerical bifurcation and path following is used to obtain global bifurcation diagrams connecting the different analytical results.

1. Introduction

The microelectronics revolution is now thirty years old and shows little sign of abating. Engineering and technological advances continue to push costs and physical sizes lower with simultaneous performance improvements. Mathematical modeling contributes to the semiconductor industry in essentially three categories: fabrication processes, device physics and circuit operation (see, for example, [1,5,6,8,9]).

This communication introduces a new topic into the last category of circuit operation. While most efforts in this area have dealt with the important problem of developing efficient numerical methods that calculate the transient behavior of large circuits with arbitrary elements, we have studied a specific circuit by various analytical and numerical methods. The *inverter ring* consists of an arbitrary number of *inverter circuits* connected together in a particular fashion (see figure 4). The inverter rings of practical interest include those with

¹ Department of Mathematical Sciences, Rensselaer Polytechnic Institute, Troy, NY 12180-3590. The research of this author was partially supported by the National Science Foundation under Grant N0. DMS-9006091.

² Department of Mathematical Sciences, Rensselaer Polytechnic Institute, Troy, NY 12180-3590. The research of these authors was supported by the National Science Foundation under Grant N0. DMS-8805539.

³ Institut für Angewandte und Numerische Mathematik, Technische Universität Wien, Wiedner Hauptstraße 8-10, 1040 Wien, Austria. The research of this author was supported by the Austrian Fonds zur Förderung der wissenschaftlichen Forschung under Grant No. J0397-PHY and by the National Science Foundation under Grant No. DMS-890813. It was carried out while this author was visiting at Rensselaer Polytechnic Institute.

an odd number of elements, called *ring oscillators*, and those with two inverters, called *flip-flops*. The ring oscillator serves two purposes. First, it is commonly employed for calibration of the intrinsic circuit speed and thus provides a key benchmark for performance of a new technology. Second, the ring oscillator is a convenient tool for converting an off-chip constant voltage to an on-chip high frequency signal. The flip-flop is used as a memory cell in static random access memories.

An example of an individual inverter circuit is shown in figure 1. It performs the binary and inherently nonlinear function of converting a high input bias to a low output bias and vice versa. The stationary characteristic function is

$$\psi_{out} = V(\psi_{in}), \quad (1.1)$$

where V maps the interval $[0, V_0]$ into itself, V_0 being the system supply bias. A typical curve for V is shown in figure 2, where the dashed line would be an ideal inverter and considered optimal by a circuit designer. In what follows, we shall make the simplifying assumption that the inverter is symmetric in the sense that

$$V(V_0 - \psi) = V_0 - V(\psi) \quad (1.2)$$

holds for the characteristic function.

As mentioned, (1.1) represents merely the static inverter characteristic. When the input varies with time, the output response will depend in a detailed fashion on the characteristics of the individual field-effect transistors (FETs) in figure 1. These characteristics are highly nonlinear and difficult to express in terms of simple equations. Instead, we propose a simple, yet representative, model of this process. Figure 3 shows the simplification in which the resistance R and the capacitance C emerge directly from FET channel resistances and loading capacitances of the inverter structure. With this simplification, the now time-dependent output bias $\psi_{out}(t)$ satisfies

$$\dot{\psi}_{out}(t) + \frac{\psi_{out}(t) - V(\psi_{in}(t))}{\tau} = 0, \quad (1.3)$$

where $\tau = RC$ is a relaxation time. Clearly, (1.1) is recovered at steady state.

The equations governing the potentials at the connection of each inverter in an inverter ring are introduced in section 2. These are an autonomous system of ordinary differential equations obtained from repeated applications of (1.3). Steady state solutions are found and their stability analyzed. The main result is that for an even number of inverters, two stable steady states exists in which the potentials are alternately 0 and V_0 . This explains the performance of the flip-flop as memory cell. It can store one bit of information

represented by one of the two stable steady states. For an odd number of inverters, i.e. the ring oscillator, one stable steady state exists for $\alpha = -V'(\frac{1}{2}V_0)$ less than a critical value, α_* say. For values greater than α_* , one expects a stable periodic solution. These are of particular interest to a circuit designer and the subsequent sections of this paper are devoted to establishing the existence of these periodic solutions which take the form of rotating waves.

In section 3, we consider an idealized problem in which the characteristic inverter function becomes a step function (as shown by the dashed line in figure 2). This simplification allows for the explicit construction of trajectories because the equations are decoupled away from discrete points in time. It is shown that rotating waves exist for every inverter ring except for $n = 2$ and $n = 4$, where n is the number of inverters. The number of rotating wave solutions is equal to the number of pairs of complex conjugate eigenvalues of an appropriate linearized problem that cross the imaginary axis as α is increased. This shows that the same number of periodic solutions emerges from Hopf bifurcations as can be constructed for the idealized problem.

Section 4 is devoted to a detailed analysis of the bifurcation at $\alpha = \alpha_*$ for ring oscillators. This is the only one of the above mentioned bifurcations which can create stable periodic solutions and, thus, it is the one of greatest practical interest. The bifurcation can be supercritical or subcritical. In the supercritical case, the bifurcating solutions are stable. Unstable solutions occur in the subcritical case. We derive a simple criterion depending on the local behavior of the characteristic function V . The standard Hopf theorem does not provide sufficient information to conclude that the bifurcating solutions are rotating waves. Therefore we employ an equivariant Hopf theorem [4] using the symmetries of the problem. This theorem guarantees that the solutions on the bifurcating branch possess spatial and temporal symmetries typical for rotating waves.

The work discussed in section 5 concerns a numerical study of the periodic solutions that emerge from the Hopf bifurcations. This study uses AUTO [3], a software package designed to follow solution branches for autonomous systems of ODEs. The connection is made between the behavior near the Hopf bifurcation (section 4) and that of the idealized problem (section 3). This section also serves as a summary of results presented in this paper.

2. The Inverter Ring and Model Equations

We shall be concerned with the circuit of n inverters as illustrated in figure 4. The goal is to model the time-dependent potentials $\psi_1(t), \dots, \psi_n(t)$ between the inverters. Since each inverter receives its input from the output of the previous inverter, repeated

applications of (1.3) generates the following system of n autonomous ordinary differential equations:

$$\dot{\psi}_j + \frac{\psi_j - V(\psi_{j-1})}{\tau} = 0, \quad j = 1, \dots, n \bmod(n). \quad (2.1)$$

Again, we take the function $V(\psi)$ to be that of figure 2.

We introduce scaled versions of the potentials and the characteristic function by

$$\begin{aligned} \psi_j^s &= \frac{2\psi_j}{V_0} - 1, \quad j = 1, \dots, n, \\ V^s(y) &= \frac{2}{V_0} V\left(\frac{V_0}{2}(y+1)\right) - 1, \end{aligned}$$

and measure time with respect to the relaxation time τ . The nondimensionalized version of (2.1) is then given by

$$\dot{\psi}_j + \psi_j - V(\psi_{j-1}) = 0, \quad j = 1, \dots, n \bmod(n), \quad (2.2)$$

where the superscript s has been dropped for notational convenience. In the scaled formulation, V maps the interval $[-1, 1]$ into itself, and the symmetry requirement (1.2) translates to the assumption that V is an odd function.

We begin by searching for steady states of (2.2) and we find it helpful to consider the discrete dynamical system corresponding to the map V . Obviously, steady states of (2.2) correspond to periodic orbits of V with period n (and these should not be confused with the periodic solutions of (2.2) to be discussed later). On the other hand, every periodic orbit with minimal period k can be used to construct k steady states for an inverter ring with n being a multiple of k . Since V is odd, we have $V(0) = 0$ and thus a trivial periodic orbit of length 1. Therefore, inverter rings with any number of elements have the trivial steady state with all potentials equal to zero.

In addition, figure 2 suggests the following assumptions on V :

$$V(1) = -1, \quad V(\psi) < -\psi \text{ for } \psi \in (0, 1). \quad (2.3)$$

An immediate consequence of the first assumption and the oddness of V is the existence of a periodic orbit of the map V with length 2. On this orbit potentials alternately take the values 1 and -1 . Therefore, every inverter ring with an even number of elements (in particular the flip-flop, but not the ring oscillator) has two more steady states with

$$\psi_j = (-1)^{j+l} \quad j = 1, \dots, n, \quad (2.4)$$

where $l = 0$ or 1 . With the above assumptions, it can be shown inductively that the k -th iterate $V^{(k)}$ of the map V satisfies

$$\begin{aligned} V^{(k)}(\psi) &< -\psi && \text{for } \psi \in (0, 1) \text{ and } k \text{ odd,} \\ V^{(k)}(\psi) &> \psi && \text{for } \psi \in (0, 1) \text{ and } k \text{ even.} \end{aligned}$$

It is easy to deduce from these properties that no additional periodic orbits of the map V , and hence steady states of (2.2), exist.

Having found all possible steady states, we now consider their stability. The inverter ring system (2.2) can be rewritten in the form

$$\dot{\Psi} + \mathbf{F}(\Psi) = \mathbf{0}, \quad (2.5)$$

where $\Psi = (\psi_1, \dots, \psi_n)^t$ and $F_j = \psi_j - V(\psi_{j-1})$ for $j = 1, \dots, n \bmod(n)$. We denote the Jacobian of \mathbf{F} evaluated at any of the above constructed steady states by \mathbf{A} and obtain

$$\mathbf{A} = \begin{pmatrix} 1 & 0 & \dots & 0 & \alpha \\ \alpha & 1 & 0 & \dots & 0 \\ 0 & \alpha & \ddots & \ddots & \vdots \\ \vdots & \ddots & \ddots & \ddots & 0 \\ 0 & \dots & 0 & \alpha & 1 \end{pmatrix}, \quad (2.6)$$

where $\alpha = -V'(0)$ ($\alpha \geq 1$) for the linearization about the trivial steady state $\Psi = \mathbf{0}$, and $\alpha = -V'(1)$ ($0 \leq \alpha \leq 1$) for the linearization about (2.4). The estimates for α follow from the assumptions (2.3) on V . The double-banded circulant matrix \mathbf{A} has different eigenvalues depending on whether n is even or odd:

$$\lambda_j = \begin{cases} 1 - \alpha e^{i2\pi(j-1)/n}, & \text{for } n \text{ even;} \\ 1 - \alpha e^{i\pi(2j-1)/n}, & \text{for } n \text{ odd.} \end{cases} \quad (2.7)$$

Stability requires that all eigenvalues have positive real part. For *even* n , $\lambda_1 = 1 - \alpha$ is the eigenvalue with the smallest real part. If we strengthen the assumptions (2.3) a little bit by requiring $V'(0) < 1$ and $V'(1) > 1$, then the trivial steady state is unstable while the steady states (2.4) are stable. For *odd* n , we only have to examine the trivial steady state. Now λ_1 and $\lambda_n = \bar{\lambda}_1$ are the eigenvalues with the smallest real parts. The condition for stability is

$$\alpha < \alpha_* = \sec \frac{\pi}{n}.$$

As indicated before, we will be more interested in the case $\alpha > \alpha_*$ in which *no* stable steady state exists and the stable solutions are periodic and take the form of rotating waves.

3. Rotating Waves for an Idealized Problem

We consider (2.2) with the idealized characteristic function

$$V(\psi) = \begin{cases} 1 & \text{for } \psi \leq 0, \\ -1 & \text{otherwise.} \end{cases}$$

Note that because of the discontinuity of V standard results for ordinary differential equations cannot be straightforwardly applied to this problem. However, no problem arises with the notion of a solution as long as our discussion remains restricted to trajectories, where solution components pass through the critical value $\psi = 0$ with nonzero speed. In this case solutions are Lipschitz continuous and the j -th potential is given by

$$\psi_j(t) = 1 + (\psi_j(t_0) - 1)e^{t_0 - t} \quad \text{or} \quad \psi_j(t) = -1 + (\psi_j(t_0) + 1)e^{t_0 - t} \quad (3.1)$$

depending on whether ψ_{j-1} is negative or positive, respectively. Therefore, the computation of trajectories can be reduced to a straightforward bookkeeping procedure keeping track of the zeros of the potentials. We try to construct rotating wave solutions, which means that the waveforms of the potentials ψ_j and ψ_{j+1} are identical up to a time shift θ independent of j :

$$\psi_{j+1}(t) = \psi_j(t + \theta) \quad j = 1, \dots, n \bmod(n)$$

Engineers refer to θ as the “delay per stage.” From $\psi_j(t) = \psi_{j+n}(t) = \psi_j(t + n\theta)$ we deduce that $n\theta$ has to be equal to an integer multiple of the period T of the rotating wave, i.e.

$$\theta = \frac{kT}{n} \quad \text{with } k \in \{1, \dots, n-1\}. \quad (3.2)$$

We look for rotating waves with a waveform as indicated in figure 5. Invoking periodicity and the assumption that the increasing and the decreasing phase are equally long implies

$$\psi_j(t) = \begin{cases} -1 + \frac{2e^{-t}}{1+e^{-T/2}} & \text{for } 0 \leq t \leq T/2, \\ 1 - \frac{2e^{T/2-t}}{1+e^{-T/2}} & \text{for } T/2 \leq t \leq T. \end{cases} \quad (3.3)$$

The time t_1 , when ψ_j decreases through zero, satisfies

$$2e^{-t_1} = 1 + e^{-T/2}. \quad (3.4)$$

At this time, ψ_{j+1} arrives at its minimum value and therefore $t_1 + \theta = T/2$ holds. This fact together with (3.2) and (3.4) provide an equation for the period T of the form

$$2e^{kT/n} = e^{T/2} + 1. \quad (3.5)$$

It is easy to show that (3.5) has a unique positive solution for T if and only if $n/4 < k < n/2$ holds. The number of rotating wave solutions is the number of integers in the open interval $(n/4, n/2)$ which, in turn, is equal to the number of pairs of complex conjugate eigenvalues with real parts smaller than one of the matrix \mathbf{A} in (2.6). This observation will be of interest below.

Because of the discontinuity of V , the stability properties of the constructed rotating waves cannot be checked by linearization of the differential equations. However, it is possible to explicitly compute smooth Poincaré maps and study the stability properties of fixed points which correspond to rotating waves. As an illustration, we apply this method to the unique rotating wave of the ring oscillator with three elements (noting that $3/4 < k = 1 < 3/2$). We consider trajectories constructed using (3.1) with initial conditions

$$\psi_1 = 0, \quad \psi_2 = x^{(0)} \in (-1, 0), \quad \psi_3 = y^{(0)} \in (0, 1).$$

When these trajectories return to the plane $\psi_1 = 0$ for the second time, the values of ψ_2 and ψ_3 are given in terms of the starting values by

$$\psi_2 = x^{(1)} = \frac{13x^{(0)} - 8y^{(0)}}{1 - 20x^{(0)} + 12y^{(0)}}, \quad \psi_3 = y^{(1)} = \frac{5y^{(0)} - 8x^{(0)}}{1 - 20x^{(0)} + 12y^{(0)}}. \quad (3.6)$$

The right hand sides of (3.6) define a map from the square $(-1, 0) \times (0, 1)$ into itself. Its fixed point

$$x = \frac{1 - \sqrt{5}}{2}, \quad y = \frac{3 - \sqrt{5}}{2}$$

corresponds to the rotating wave solution constructed above. The stability of (x, y) can be checked by computing the eigenvalues of the Jacobian of (3.6) evaluated at (x, y) . It turns out that both eigenvalues have moduli smaller than one implying stability of the rotating wave.

An analogous procedure can be carried out for $n > 3$, but the necessary algebra is rather involved. Instead, we defer a further discussion of the stability to sections 4 and 5. The analysis of section 4 and the numerical examples in section 5 suggest the conjecture that for even n all rotating wave solutions are unstable, whereas for odd n there is one stable rotating wave corresponding to $k = \frac{n-1}{2}$ in the above construction.

4. Rotating Waves from an Equivariant Hopf Theorem

Our aim in this section is to study the bifurcation to rotating waves. From the linear analysis of section 2, it would appear that a standard Hopf bifurcation (without symmetries) is involved here. But the standard Hopf theorem [4] is not rich enough to account

for rotating waves. It is a phenomenon that involves not only spatial symmetries but also an interplay of temporal symmetry. Hence, we require the richer $Z_n \times S^1$ -equivariant Hopf theorem, which takes into consideration the interplay of the cyclic group of spatial symmetries Z_n and phase shifts S^1 .

We shall restrict our study to symmetric Hopf bifurcations at α_* for the ring oscillator (n odd). A similar analysis holds when n is even and at subsequent bifurcations.

First, we show that (2.5) has the spatial symmetries of the cyclic group Z_n ; in other words, (2.5) is Z_n -equivariant,

$$\mathbf{F}(\xi^k \Psi; \alpha) = \xi^k \mathbf{F}(\Psi; \alpha) \quad \text{for any element } \xi^k \in Z_n, k \in \{1, \dots, n\}, \quad (4.1)$$

where we have now included the bifurcation parameter $\alpha = V'(0)$ into the definition of \mathbf{F} . The generator ξ has the symmetry of a regular n -gon, i.e.

$$\xi(\psi_1, \dots, \psi_n)^t = (\psi_2, \dots, \psi_n, \psi_1)^t.$$

Hence, (4.1) follows because

$$F_j(\xi \Psi; \alpha) = \psi_{j+1} - V(\psi_j) = F_{j+1}(\Psi; \alpha).$$

Thus, \mathbf{F} is Z_n -equivariant.

It is not enough to consider only the simple Z_n -equivariant Hopf bifurcation [4]. The very nature of rotating waves requires the interplay of Z_n symmetry and the S^1 group of phase shifts.

We consider the following joint action of $(\xi^k, \theta) \in Z_n \times S^1$:

$$(\xi^k, \theta)\Psi(t) = \xi^k \Psi(t + \theta). \quad (4.2)$$

The rotating waves in a ring oscillator can be described as follows: the waveform at inverter j phase-shifted by $\theta = \frac{kT}{n}$ coincides with the waveform at inverter $j + k \bmod(n)$. That is,

$$(\psi_{1+k}(t), \dots, \psi_{n+k}(t)) = (\psi_1(t + \theta), \dots, \psi_n(t + \theta)). \quad (4.3)$$

This is exactly the same symmetries present in the idealized problem of section 3. In terms of the action (4.2), we write (4.3) as

$$(\xi^k, \theta)\Psi(t) = \xi^k \Psi(t + \theta) = \Psi(t - \theta + \theta) = \Psi(t),$$

which means that a rotating wave $\Psi(t)$ is a fixed point of (4.2).

We now proceed to describe the $Z_n \times S^1$ -Hopf bifurcation. By the usual equivariant Lyapunov-Schmidt reduction procedure carried out carefully using invariant complements the reduced bifurcation equation is $Z_n \times S^1$ -equivariant (cf. [4], pp. 300-308). The periodic solutions that bifurcate from the trivial branch $\Psi = \mathbf{0}$ of (2.5) correspond to the nontrivial zeros of

$$\phi(x, y; \alpha, s) = p(x^2 + y^2, \alpha, s) \begin{pmatrix} x \\ y \end{pmatrix} + q(x^2 + y^2, \alpha, s) \begin{pmatrix} -y \\ x \end{pmatrix}, \quad (4.4)$$

in a two-dimensional space with coordinates (x, y) . This two-dimensional space is typically invariant under some isotropy subgroup $\Sigma \subset Z_n \times S^1$. (More will be said on this point later.) The variable s in (4.4) gives the period $T = 2\pi/[(1+s)\tan\frac{\pi}{n}]$ of the bifurcating solutions. The form of (4.4) in terms of the smooth functions p and q , which depend on (x, y) through the radius $x^2 + y^2$, is prescribed by the fact that the reduced equation for ϕ must commute with phase shifts S^1 [4].

Note that (4.4) implies that $\phi = 0$ if and only if one of the following holds:

$$x = y = 0 \quad \text{or} \quad p = q = 0.$$

The first solution corresponds to the trivial branch of solutions $\Psi = \mathbf{0}$, while the second corresponds to nonconstant periodic solutions of (2.5) provided $x^2 + y^2 \neq 0$. Let us define $\sigma = x^2 + y^2$, and we shall be interested in the case

$$p(\sigma, \alpha, s) = 0, \quad (4.5a)$$

$$q(\sigma, \alpha, s) = 0. \quad (4.5b)$$

In order to solve (4.5), we need the usual properties for Hopf bifurcation; namely,

$$p(0, \alpha_*, 0) = 0, \quad (4.6a)$$

$$q(0, \alpha_*, 0) = 0, \quad (4.6b)$$

$$p_s(0, \alpha_*, 0) = 0, \quad (4.6c)$$

$$q_s(0, \alpha_*, 0) \neq 0, \quad (4.6d)$$

$$p_\alpha(0, \alpha_*, 0) \neq 0, \quad (4.6e)$$

where $\alpha_* = \sec\frac{\pi}{n}$. Properties (4.6a,b,c,d) are established in [4], while (4.6e) is equivalent to the condition that the eigenvalue pair (λ_1, λ_n) from (2.7) cross the imaginary axis with nonzero speed at $\alpha = \alpha_*$. One solves for $s = s(\sigma, \alpha)$ from (4.5b) using the pair of equations (4.6b,d) and the implicit function theorem. Upon substitution into (4.5a), we obtain the final bifurcation equation

$$r(\sigma, \alpha) \equiv p(\sigma, \alpha, s(\sigma, \alpha)) = 0. \quad (4.7)$$

Then, we obtain $\alpha = \alpha(\sigma)$, where $\alpha_* = \alpha(0)$, from (4.7) using (4.6e) and the implicit function theorem.

Whether the Hopf bifurcation is supercritical or subcritical depends on whether $\frac{d\alpha}{d\sigma}$ is positive or negative, respectively. This condition translates to a condition on the sign of $V'''(0)$, which we will now show. (Recall that the second derivative of V is zero at $\psi = 0$ since we have assumed that V is an odd function.)

Upon differentiating (4.7) with respect to σ and setting $\sigma = 0$, we find

$$\frac{d\alpha}{d\sigma} = -\frac{r_\sigma(0, \alpha_*)}{r_\alpha(0, \alpha_*)}. \quad (4.8)$$

From the linear analysis in section 2 and the fact that $r_\alpha(0, \alpha_*)$ is the rate at which (λ_1, λ_n) cross the imaginary axis, we find

$$r_\alpha(0, \alpha_*) = -\cos \frac{\pi}{n}. \quad (4.9)$$

The numerator $r_\sigma(0, \alpha_*)$ in (4.8) can be computed in terms of the vector field \mathbf{F} in (2.5) (cf. [4], p. 352, modulo suitable changes in scalings and notation) from

$$r_\sigma(0, \alpha_*) = \frac{1}{4} \operatorname{Re} \{ Y^t \mathbf{F}'''(X, X, \bar{X}) \}, \quad (4.10)$$

where \mathbf{F}''' denotes the third (Fréchet) derivative of \mathbf{F} with respect to Ψ evaluated at $(\Psi, \alpha) = (\mathbf{0}, \alpha_*)$, and $X, Y \in \mathbb{C}^n$ satisfy

$$\begin{aligned} \mathbf{A}_* X &= i\mu X, & \bar{X}^t X &= 1, \\ \mathbf{A}_*^t Y &= i\mu Y, & \bar{Y}^t Y &= 1. \end{aligned}$$

The real matrix \mathbf{A}_* is given by (2.6) and $\mu \equiv \operatorname{Im} \lambda_n$ both evaluated at $\alpha = \alpha_*$.

A straightforward calculation shows that

$$X_j = \frac{(-1)^j}{\sqrt{n}} e^{ij\pi/n} \quad \text{and} \quad Y_j = \frac{(-1)^j}{\sqrt{n}} e^{-ij\pi/n}, \quad (4.11)$$

Also, for any $A, B, C \in \mathbb{C}^n$

$$\mathbf{F}'''(A, B, C) = -V'''(0)(A_n B_n C_n, A_1 B_1 C_1, \dots, A_{n-1} B_{n-1} C_{n-1})^t. \quad (4.12)$$

Hence, from (4.10), (4.11) and (4.12), we find

$$r_\sigma(0, \alpha_*) = \frac{V'''(0)}{4n} \cos \frac{\pi}{n}. \quad (4.13)$$

Finally, (4.13) along with (4.9) in (4.8) gives

$$\frac{d\alpha}{d\sigma} = \frac{V'''(0)}{4n}.$$

The final result, as indicated before, is that when

$$V'''(0) > 0, \quad \text{the bifurcation is supercritical,}$$

and when

$$V'''(0) < 0, \quad \text{the bifurcation is subcritical.}$$

This result also determines the stability of the bifurcating periodic solutions. Because the form of the reduced equation $\phi = 0$ (4.4) is the same as in the standard Hopf theorem, the periodic solution is orbitally asymptotically stable if $V'''(0) > 0$ and vice versa.

We are now ready to discuss the symmetries of the bifurcating periodic solutions whose existence and stability are discussed above. Recall from the beginning of this section that the nontrivial periodic solutions of (2.5) correspond to the nontrivial zeros of (4.4) in the two-dimensional fixed point space of some isotropy subgroup $\Sigma \subset Z_n \times S^1$.

We require the two-dimensional irreducible representations ρ_m of Z_n on the complex numbers \mathbb{C} [7]. Let $w = e^{i2\pi/n}$ and let ξ be a generator of Z_n . Then they are

$$\xi z = w^m z, \quad m = 1, 2, \dots, \frac{n-1}{2}. \quad (4.14)$$

Consider the $Z_n \times S^1$ action on \mathbb{C} given by

$$(\xi^k, \theta)z = w^{mk} e^{i\theta} z, \quad k = \{1, \dots, n\}, \quad (4.15)$$

where the positive angle θ has been selected by reversing time if necessary. Note that this action (4.15) corresponds to the action (4.2) of $Z_n \times S^1$ on periodic functions $\Psi(t)$.

The only subgroup $\Sigma \subset Z_n \times S^1$ with two-dimensional fixed point space is the kernel of $Z_n \times S^1$, i.e.

$$\Sigma_m = \{(\xi^k, \theta) \in Z_n \times S^1 \mid w^{mk} e^{i\theta} = 1\}.$$

Since $\frac{2\pi mk}{n} + \theta = 0$, we have

$$\Sigma_m = \left\{ \left(\xi^k, -\frac{2\pi mk}{n} \right) \mid k = 1, \dots, n \right\},$$

which is isomorphic to Z_n .

Thus for each two-dimensional representation ρ_m (4.14), $m = 1, \dots, \frac{n-1}{2}$, there is a unique one-parameter family of periodic solutions with periods close to $2\pi / \tan \frac{\pi}{n}$ such that

they are fixed points of Σ_m in the action (4.15). In other words, for $m = 1, \dots, \frac{n-1}{2}$, each family of periodic solutions parametrized by α is made up of unidirectional rotating waves of type Σ_m . The unidirectional nature comes from the fact that the positive angle θ was selected by fixing the direction of time in (4.15).

5. Numerical Path Following of Rotating Waves

We now perform a numerical study of the system of ODEs (2.5) with a specific function $V(\psi)$ in order to illustrate the results of sections 3 and 4. We show that the periodic solutions for $\alpha \rightarrow \infty$ (section 3) are the limiting solutions along the branches of periodic solutions that emerge from a sequence of Hopf bifurcations (the first of which having been examined in section 4). The tool used in this study is the software package AUTO [3], which employs a numerical continuation procedure to calculate solution branches for autonomous systems of ODEs and determines limit (or fold) points and bifurcation points along these branches.

We begin by choosing a specific $V(\psi)$. Recall from (2.2) that

$$\dot{\psi}_j + \psi_j - V(\psi_{j-1}) = 0, \quad j = 1, \dots, n \bmod(n),$$

where V has the form shown in figure 2, but in our scaled formulation V maps the interval $[-1, 1]$ into itself and we have assumed that V is odd. We choose

$$V(\psi) = -\tanh\left(\alpha\psi + \left(\frac{\alpha^3}{3} - \beta\right)\psi^3\right). \quad (5.1)$$

With this choice, $\alpha = V'(0)$ is the same bifurcation parameter as that used in section 4 and the sign of $\beta = \frac{V'''(0)}{6}$ will control whether the Hopf bifurcations are supercritical or subcritical. Also, V approaches the idealized characteristic function (a step function) as $\alpha \rightarrow \infty$. It should be noted that the assumptions (2.3) are not satisfied for all values of α, β . Figure 6 shows V versus ψ for various values of α, β .

The procedure for calculating the solution branches for a ring oscillator with n inverters is the following: we begin on the trivial branch $\Psi = \mathbf{0}$ with $\alpha = 1 < \alpha_*$ and some (fixed) value of β , $\beta = 1$ or -1 say. We follow the trivial branch as α increases and record the sequence of Hopf bifurcations. The number of bifurcations is equal to the number of eigenvalue pairs $(\lambda_j, \lambda_{n+1-j})$ given in (2.7) that can cross the imaginary axis as α increases (as discussed in section 3). At each Hopf bifurcation a branch of periodic solutions emerges. Each of these branches is followed as α, T varies, where T is the period.

In figure 7, we show two typical bifurcation diagrams, one for $\beta = 1$ and the other for $\beta = -1$. In this case, we have chosen $n = 7$ so that two Hopf bifurcations are anticipated

along the trivial solution branch. For $\beta > 0$ (figure 7(a)), the Hopf bifurcations are indeed supercritical as predicted in section 4. The values of α increase from the two bifurcation points and continue to increase along each branch (for our choice of V). The periodic solutions that emerge from the first Hopf bifurcation at $\alpha_* = \sec \frac{\pi}{7} = 1.11$ are stable (as indicated by the solid curve), whereas the solutions that bifurcate from the second Hopf bifurcation are unstable (as indicated by the dashed curve). For this second branch of periodic solutions, the trivial branch has no stability to give away. For $\beta < 0$ (figure 7(b)), the Hopf bifurcations are subcritical. The values of α first decrease (only slightly) from the bifurcation point, then increase upon passage through a limit point, where an exchange of stability occurs for the first bifurcated branch. Figure 8 is an enlarged view of the curves in figure 7 near α_* that clearly shows the behavior of the solution branches near the first Hopf bifurcation.

The waveform at various points along the solution branches for $\beta = -1$ (figure 7(b)) are shown in figure 9. In this plot, we see clearly the approach to the idealized solutions of section 3 (as shown by the dashed curves).

References

- [1] K. Board and D. R. J. Owen, eds., *Simulation of Semiconductor Devices and Processes*, Pineridge Press, Swansea, 1984.
- [2] S.N. Chow and J.K. Hale, *Methods of Bifurcation Theory*, Springer-Verlag, New York, 1982.
- [3] E. Doedel, *AUTO 86 user manual*, Caltech Applied Mathematics Report, 1988.
- [4] M. Golubitsky and D.G. Schaeffer, *Singularities and Groups in Bifurcation Theory, Vols. I and II*, Springer-Verlag, New York, 1985.
- [5] P. A. Markowich, *The Stationary Semiconductor Device Equations*, Springer-Verlag, Wien, 1986.
- [6] P. A. Markowich, C. Ringhofer and C. Schmeiser, *Semiconductor Equations*, Springer-Verlag, Wien, 1990.
- [7] W. Miller, *Symmetry Groups and their Applications*, Academic Press, New York, 1972.
- [8] M.S. Mock, *Analysis of Mathematical Models of Semiconductor Devices*, Boole Press, Dublin, 1983.
- [9] P.W. Tuinenga, *SPICE: A Guide to Circuit Simulation and Analysis using PSPICE*, Prentice-Hall, Englewood Cliffs, 1988.

Figure Captions

Figure 1 CMOS inverter circuit.

Figure 2 Characteristic inverter output curve.

Figure 3 Simplified inverter circuit.

Figure 4 Inverter ring circuit.

Figure 5 Waveform of rotating waves for idealized inverter rings.

Figure 6 Characteristic function (5.1).

Figure 7 Bifurcation diagram for $n = 7$; (a) $\beta = 1$, (b) $\beta = -1$.

Figure 8 Behavior near α_* .

Figure 9 Waveforms along the solution branches for $\beta = -1$.

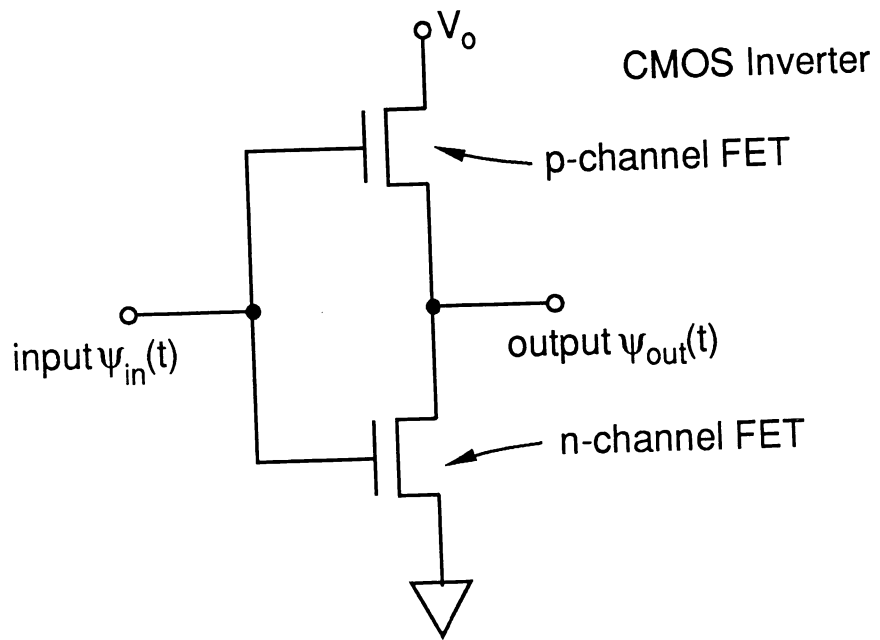


Fig. 1

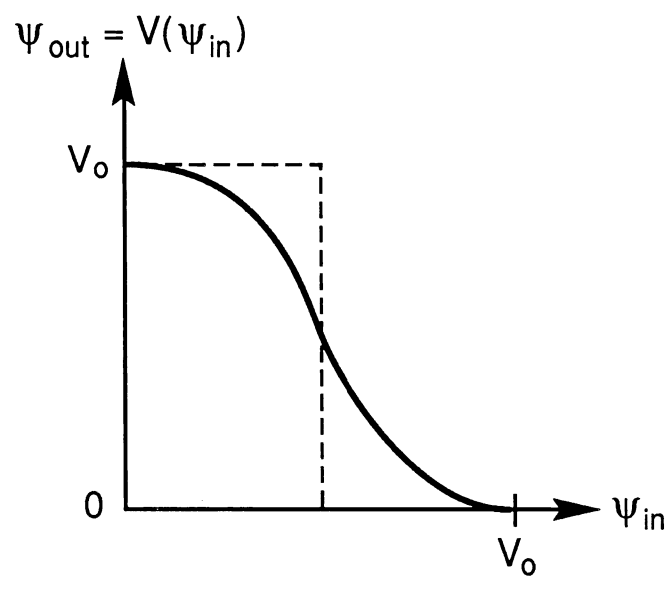
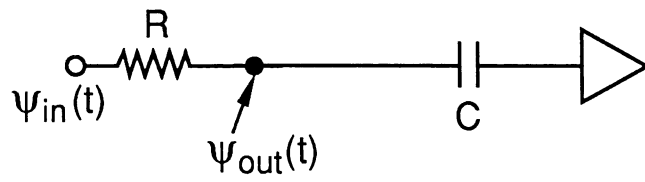
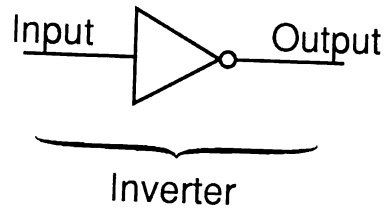
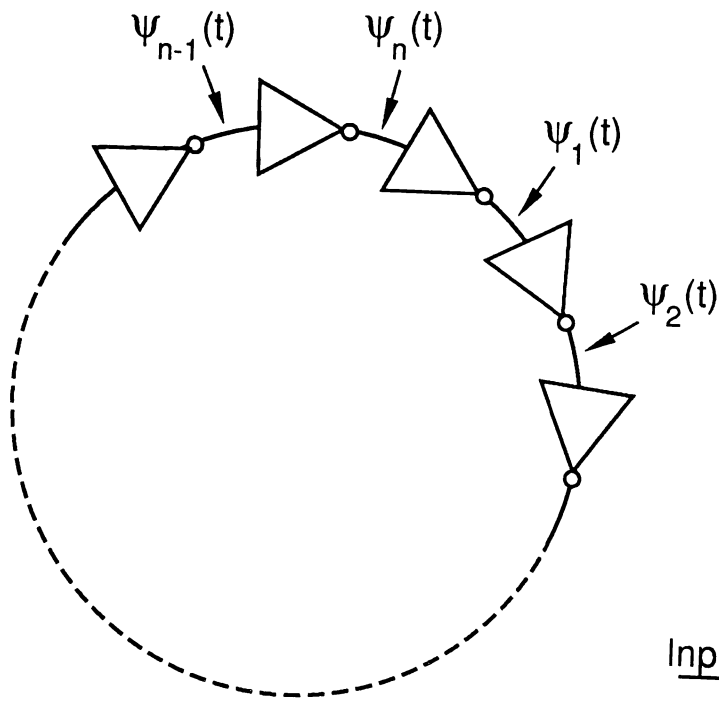
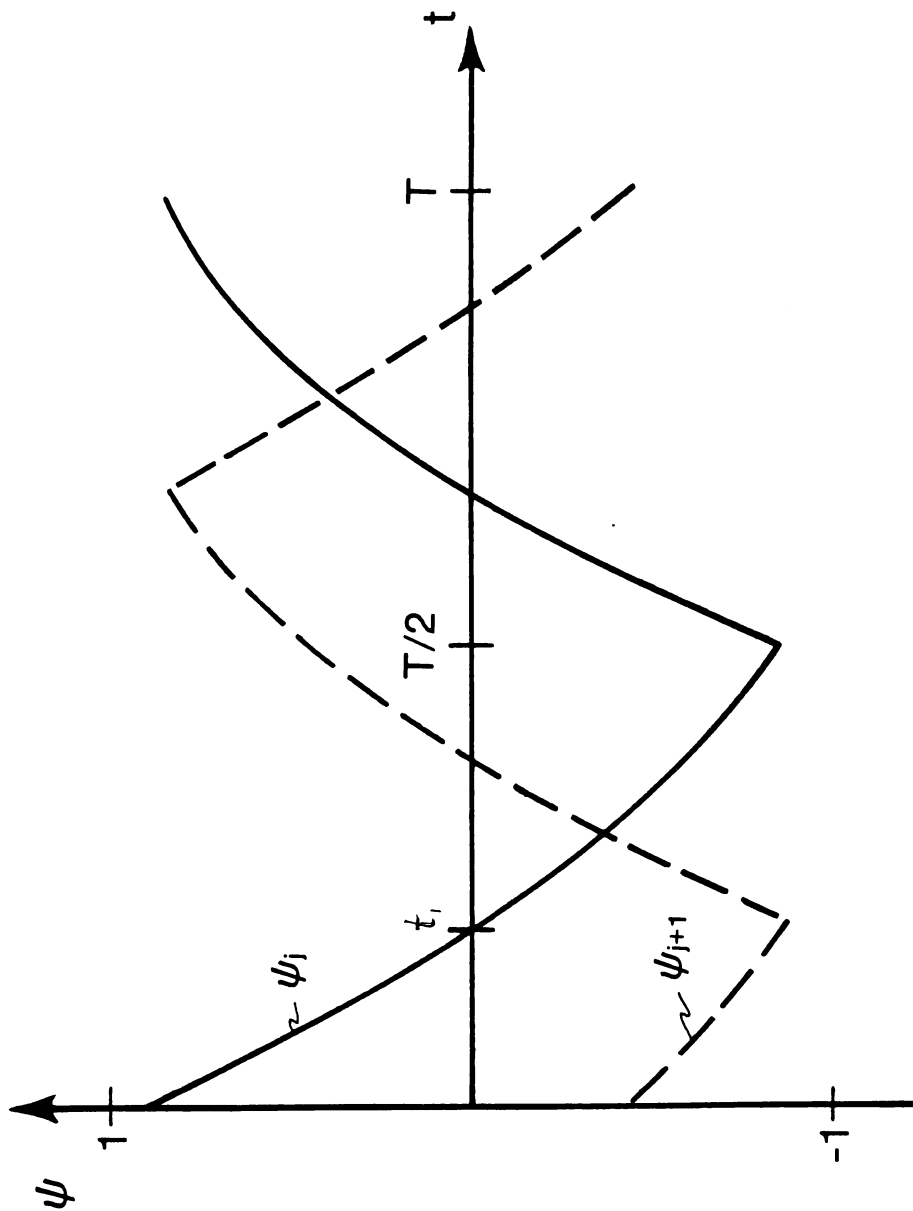
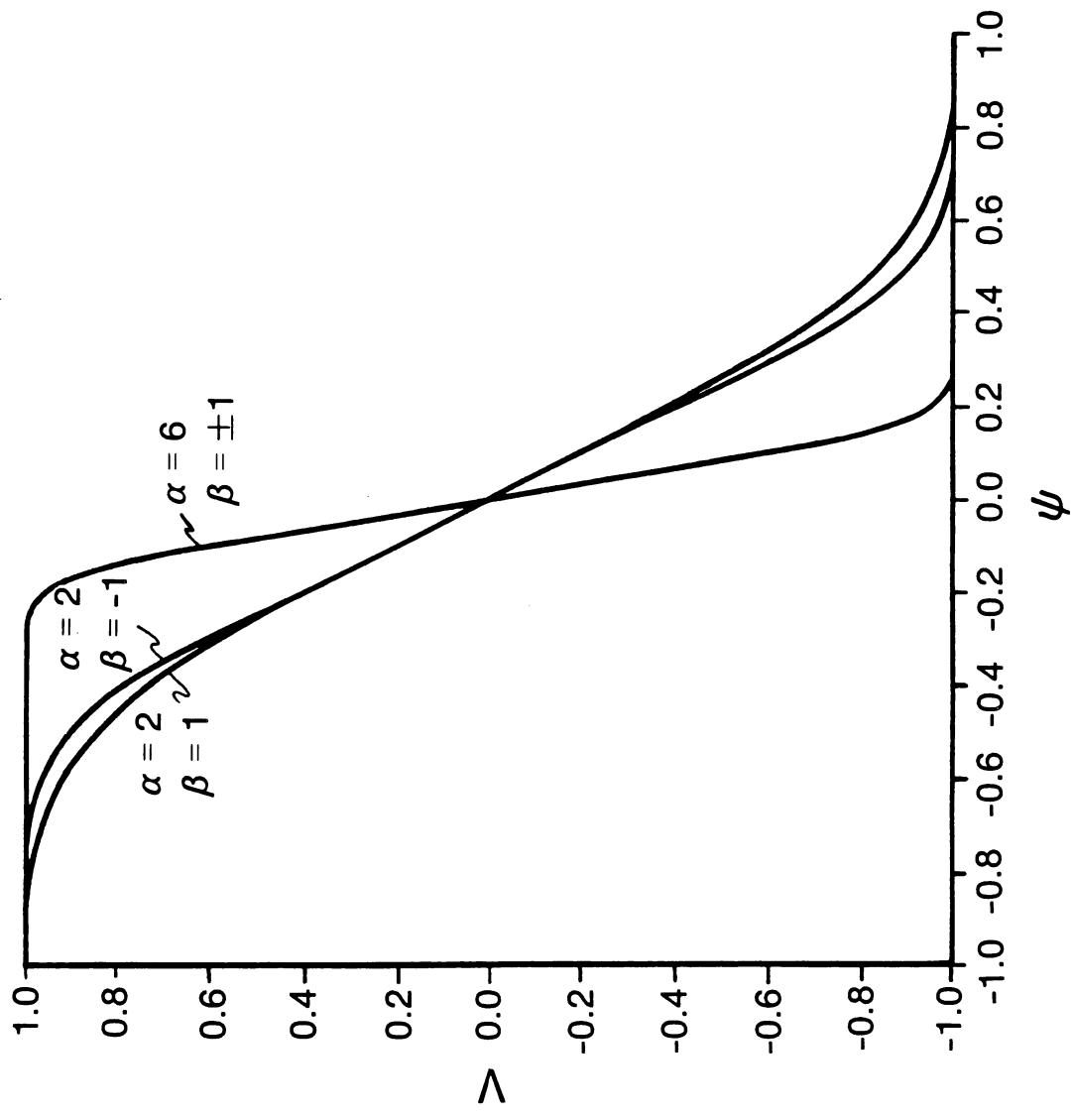


Fig. 2









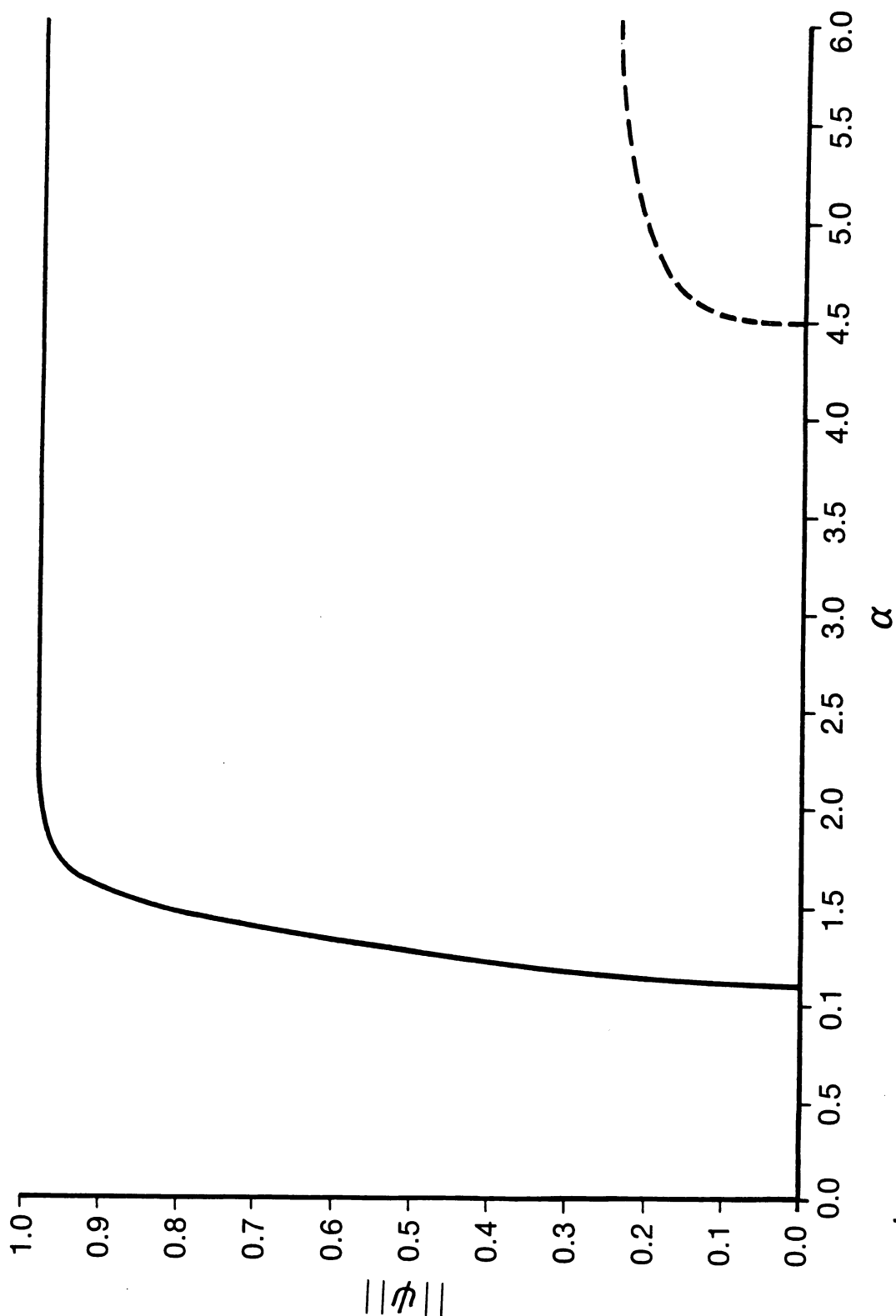


Fig. 7(a)

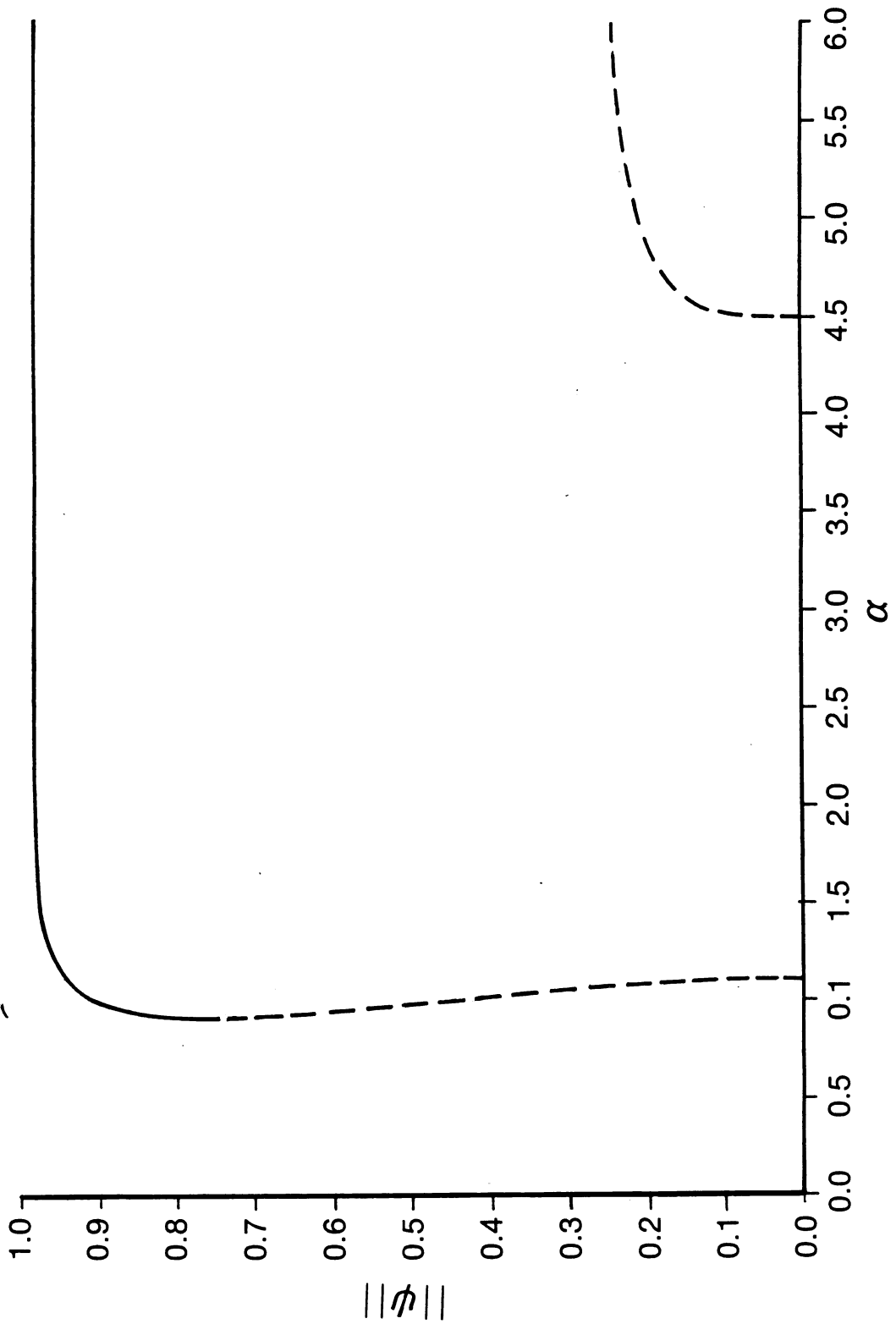
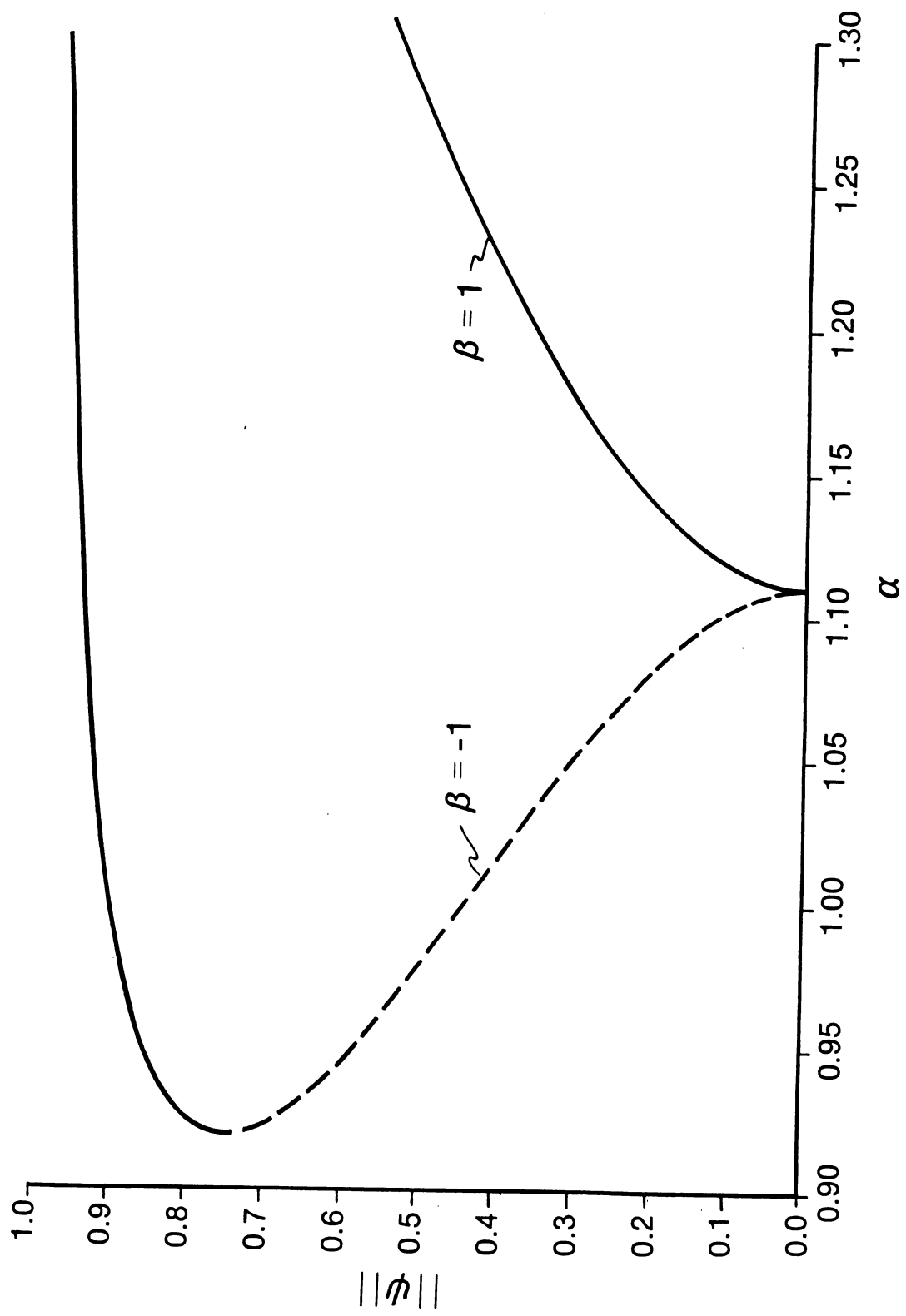
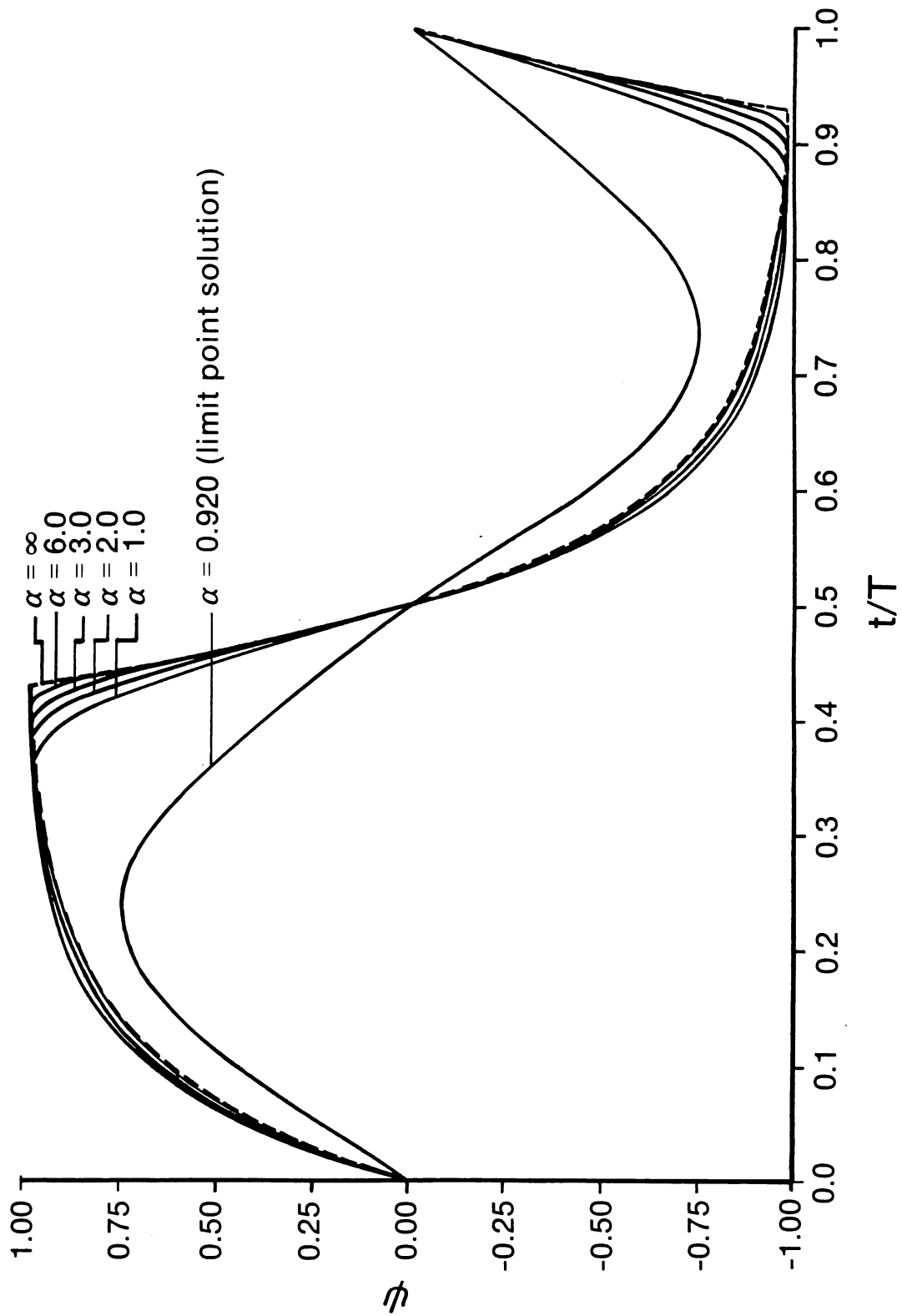


Fig. 7(b)





Recent IMA Preprints

#	Author/s	Title
637	Xinfu Chen,	Generation and propagation of the interface for reaction–diffusion equations
638	Philip Korman,	Dynamics of the Lotka–Volterra systems with diffusion
639	Harlan W. Stech,	Generic Hopf bifurcation in a class of integro-differential equations
640	Stephane Laederich,	Periodic solutions of non linear differential difference equations
641	Peter J. Olver,	Canonical Forms and Integrability of BiHamiltonian Systems
642	S.A. van Gils, M.P. Krupa and W.F. Langford,	Hopf bifurcation with nonsemisimple 1:1 Resonance
643	R.D. James and D. Kinderlehrer,	Frustration in ferromagnetic materials
644	Carlos Rocha,	Properties of the attractor of a scalar parabolic P.D.E.
645	Debra Lewis,	Lagrangian block diagonalization
646	Richard C. Churchill and David L. Rod,	On the determination of Ziglin monodromy groups
647	Xinfu Chen and Avner Friedman,	A nonlocal diffusion equation arising in terminally attached polymer chains
648	Peter Gritzmann and Victor Klee,	Inner and outer j - Radii of convex bodies in finite- dimensional normed spaces
649	P. Szmolyan,	Analysis of a singularly perturbed traveling wave problem
650	Stanley Reiter and Carl P. Simon,	Decentralized dynamic processes for finding equilibrium
651	Fernando Reitich,	Singular solutions of a transmission problem in plane linear elasticity for wedge-shaped regions
652	Russell A. Johnson,	Cantor spectrum for the quasi-periodic Schrödinger equation
653	Wenxiong Liu,	Singular solutions for a convection diffusion equation with absorption
654	Deborah Brandon and William J. Hrusa,	Global existence of smooth shearing motions of a nonlinear viscoelastic fluid
655	James F. Reineck,	The connection matrix in Morse–Smale flows II
656	Claude Baesens, John Guckenheimer, Seunghwan Kim and Robert Mackay,	Simple resonance regions of torus diffeomorphisms
657	Willard Miller, Jr.,	Lecture notes in radar/sonar: Topics in Harmonic analysis with applica- tions to radar and sonar
658	Calvin H. Wilcox,	Lecture notes in radar/sonar: Sonar and Radar Echo Structure
659	Richard E. Blahut,	Lecture notes in radar/sonar: Theory of remote surveillance algorithms
660	D.V. Anosov,	Hilbert’s 21st problem (according to Bolibruch)
661	Stephane Laederich,	Ray–Singer torsion for complex manifolds and the adiabatic limit
662	Geneviève Raugel and George R. Sell,	Navier-Stokes equations in thin 3d domains: Global regularity of solutions I
663	Emanuel Parzen,	Time series, statistics, and information
664	Andrew Majda and Kevin Lamb,	Simplified equations for low Mach number combustion with strong heat release
665	Ju. S. Il’yashenko,	Global analysis of the phase portrait for the Kuramoto–Sivashinsky equation
666	James F. Reineck,	Continuation to gradient flows
667	Mohamed Sami Elbially,	Simultaneous binary collisions in the collinear N -body problem
668	John A. Jacquez and Carl P. Simon,	Aids: The epidemiological significance of two different mean rates of partner-change
669	Carl P. Simon and John A. Jacquez,	Reproduction numbers and the stability of equilibria of SI models for heterogeneous populations
670	Matthew Stafford,	Markov partitions for expanding maps of the circle
671	Ciprian Foias and Edriss S. Titi,	Determining nodes, finite difference schemes and inertial manifolds
672	M.W. Smiley,	Global attractors and approximate inertial manifolds for abstract dissipative equations
673	M.W. Smiley,	On the existence of smooth breathers for nonlinear wave equations
674	Hitay Özbay and Janos Turi,	Robust stabilization of systems governed by singular integro-differential equations
675	Mary Silber and Edgar Knobloch,	Hopf bifurcation on a square lattice
676	Christophe Golé,	Ghost circles for twist maps
677	Christophe Golé,	Ghost tori for monotone maps
678	Christophe Golé,	Monotone maps of $T^n \times R^n$ and their periodic orbits
679	E.G. Kalnins and W. Miller, Jr.,	Hypergeometric expansions of Heun polynomials
680	Victor A. Pliss and George R. Sell,	Perturbations of attractors of differential equations
681	Avner Friedman and Peter Knabner,	A transport model with micro- and macro-structure
682	E.G. Kalnins and W. Miller, Jr.,	A note on group contractions and radar ambiguity functions
683	George R. Sell,	References on dynamical systems
684	Shui-Nee Chow, Kening Lu and George R. Sell,	Smoothness of inertial manifolds
685	Shui-Nee Chow, Xiao-Biao Lin and Kening Lu,	Smooth invariant foliations in infinite dimensional spaces

- 686 **Kening Lu**, A Hartman–Grobman theorem for scalar reaction-diffusion equations
- 687 **Christophe Golé and Glen R. Hall**, Poincaré’s proof of Poincaré’s last geometric theorem
- 688 **Mario Taboada**, Approximate inertial manifolds for parabolic evolutionary equations via Yosida approximations
- 689 **Peter Rejto and Mario Taboada**, Weighted resolvent estimates for Volterra operators on unbounded intervals
- 690 **Joel D. Avrin**, Some examples of temperature bounds and concentration decay for a model of solid fuel combustion
- 691 **Susan Friedlander and Misha M. Vishik**, Lax pair formulation for the Euler equation
- 692 **H. Scott Dumas**, Ergodization rates for linear flow on the torus
- 693 **A. Eden, A.J. Milani and B. Nicolaenko**, Finite dimensional exponential attractors for semilinear wave equations with damping
- 694 **A. Eden, C. Foias, B. Nicolaenko & R. Temam**, Inertial sets for dissipative evolution equations
- 695 **A. Eden, C. Foias, B. Nicolaenko & R. Temam**, Hölder continuity for the inverse of Mañé’s projection
- 696 **Michel Chipot and Charles Collins**, Numerical approximations in variational problems with potential wells
- 697 **Huanan Yang**, Nonlinear wave analysis and convergence of MUSCL schemes
- 698 **László Gerencsér and Zsuzsanna Vágó**, A strong approximation theorem for estimator processes in continuous time
- 699 **László Gerencsér**, Multiple integrals with respect to L -mixing processes
- 700 **David Kinderlehrer and Pablo Pedregal**, Weak convergence of integrands and the Young measure representation
- 701 **Bo Deng**, Symbolic dynamics for chaotic systems
- 702 **P. Galdi, D.D. Joseph, L. Preziosi, S. Rionero**, Mathematical problems for miscible, incompressible fluids with Korteweg stresses
- 703 **Charles Collins and Mitchell Luskin**, Optimal order error estimates for the finite element approximation of the solution of a nonconvex variational problem
- 704 **Peter Gritzmann and Victor Klee**, Computational complexity of inner and outer j -radii of polytopes in finite-dimensional normed spaces
- 705 **A. Ronald Gallant and George Tauchen**, A nonparametric approach to nonlinear time series analysis: estimation and simulation
- 706 **H.S. Dumas, J.A. Ellison and A.W. Sáenz**, Axial channeling in perfect crystals, the continuum model and the method of averaging
- 707 **M.A. Kaashoek and S.M. Verduyn Lunel**, Characteristic matrices and spectral properties of evolutionary systems
- 708 **Xinfu Chen**, Generation and Propagation of interfaces in reaction diffusion systems
- 709 **Avner Friedman and Bei Hu**, Homogenization approach to light scattering from polymer-dispersed liquid crystal films
- 710 **Yoshihisa Morita and Shuichi Jimbo**, ODEs on inertial manifolds for reaction-diffusion systems in a singularly perturbed domain with several thin channels
- 711 **Wenxiong Liu**, Blow-up behavior for semilinear heat equations: multi-dimensional case
- 712 **Hi Jun Choe**, Hölder continuity for solutions of certain degenerate parabolic systems
- 713 **Hi Jun Choe**, Regularity for certain degenerate elliptic double obstacle problems
- 714 **Fernando Reitich**, On the slow motion of the interface of layered solutions to the scalar Ginzburg–Landau equation
- 715 **Xinfu Chen and Fernando Reitich**, Local existence and uniqueness of solutions of the Stefan problem with surface tension and kinetic undercooling
- 716 **C.C. Lim, J.M. Pimbley, C. Schmeiser and D.W. Schwendeman**, Rotating waves for semiconductor inverter rings
- 717 **W. Balsler, B.L.J. Braaksma, J.-P. Ramis and Y. Sibuya**, Multisummability of formal power series solutions of linear ordinary differential equations
- 718 **Peter J. Olver and Chehrzad Shakiban**, Dissipative decomposition of partial differential equations
- 719 **Clark Robinson**, Homoclinic bifurcation to a transitive attractor of Lorenz type, II
- 720 **Michelle Schatzman**, A simple proof of convergence of the QR algorithm for normal matrices without shifts
- 721 **Ian M. Anderson, Niky Kamran and Peter J. Olver**, Internal, external and generalized symmetries
- 722 **C. Foias and J.C. Saut**, Asymptotic integration of Navier–Stokes equations with potential forces. I
- 723 **Ling Ma**, The convergence of semidiscrete methods for a system of reaction-diffusion equations
- 724 **Adelina Georgescu**, Models of asymptotic approximation
- 725 **A. Makagon and H.Salehi**, On bounded and harmonizable solutions on infinite order arma systems
- 726 **San-Yih Lin and Yan-Shin Chin**, An upwind finite-volume scheme with a triangular mesh for conservation laws
- 727 **J.M. Ball, P.J. Holmes, R.D. James, R.L. Pego & P.J. Swart**, On the dynamics of fine structure
- 728 **KangPing Chen and Daniel D. Joseph**, Lubrication theory and long waves